Advances in Materials Technology for Fossil Power Plants
Proceedings from the Sixth International Conference
August 31–September 3, 2010, Santa Fe, New Mexico, USA
https://doi.org/10.31399/asm.cp.am-epri-2010p0268

D. Gandy, J. Shingledecker, R. Viswanathan, editors

Online Gas Measurements in a Pilot-Scale Combustion Facility for Fireside Corrosion Study

Steven C. Kung

Materials & Manufacturing Technology
Babcock & Wilcox Power Generation Group
20 South Van Buren Avenue
Barberton, OH 44203
Email: sckung@babcock.com

ABSTRACT

A comprehensive fireside corrosion study was undertaken to better understand the corrosion mechanisms operating on the superheaters and lower furnace walls of advanced coal-fired utility boilers. The study intended to evaluate the fireside conditions generated from burning eight U.S. coals individually in a pilot-scale combustion facility. These coals consisted of a wide range of compositions that are of interest to the utility industry. The combustion facility was capable of producing the realistic conditions of staged combustion existing in coal-fired utility boilers. During each of the combustion tests, gas and deposit samples were collected and analyzed via in-furnace probing at selected locations corresponding to the waterwalls and superheaters. Testing of five of the eight coal groups has been completed to date. Results of these online measurements helped reveal the dynamic nature of the combustion environments produced in coal-fired boilers. Coexistence of reducing and oxidizing species in the gas phase was evident in both combustion zones, indicating that thermodynamic equilibrium of the overall combustion gases was generally unattainable. However, the amount of sulfur released from coal to form sulfur-bearing gaseous species in both the reducing and oxidizing zones was in a linear relationship with the amount of the total sulfur in coal, independent of the original sulfur forms. Such a linear relationship was also observed for the measured HCl gas relative to the coal chlorine content. However, the release of sulfur from coal to the gas phase appeared to be slightly faster and more complete than that of chlorine in the combustion zone, while both sulfur and chlorine were completely released and reacted to form respective gaseous species in the oxidizing zone. The information of sulfur and chlorine release processes in coal combustion generated from this study is considered new to the industry and provides valuable insight to the understanding of fireside corrosion mechanisms.

INTRODUCTION

The recent development of high-efficiency and low-emission coal-fired utility boilers has led to the conditions of higher steam temperatures and pressures.[1] The design strategies of these boilers often involve implementation of staged combustion that produces corrosive combustion gases in the lower furnace. In addition, the higher steam conditions will inevitably require the use of high-temperature creep and corrosion resistant alloys for superheater/reheater in the upper furnace. Examples include the development of ultra supercritical (USC) boiler systems that will push the steam outlet temperatures up to 760°C (1400°F) at pressures up to 35 MPa (5000 psi). While a higher efficiency, and thus lower CO_2 emission on a per megawatt basis, can be realized from these advanced combustion systems, accelerated fireside corrosion is also anticipated on the boiler tubes. For instance, low-NO_X combustion produces H_2S in the flue gas and FeS in the deposit from incomplete combustion of the sulfur in coal. Both of these sulfide species are known to increase fireside corrosion on the lower furnace walls via sulfidation, although the corrosion mechanisms are distinctly different.[2-4] Utility boilers retrofitted with low-NO_X burners and/or implemented staged combustion in recent years have indeed experienced accelerated tube wastage in the lower furnace. Consequently, application of coatings or weld overlays is often required to protect the waterwalls from accelerated corrosion wastage. As the metal temperatures of furnace walls are expected to increase in the advanced boiler systems, sulfidation attack will likely be further intensified as well. In the upper furnace, higher steam temperatures will raise the metal temperatures of superheaters and reheaters, thus increasing the propensity for coal ash corrosion (also known as hot corrosion).[5] The highest coal ash corrosion attack will likely occur on tubes operating at intermediate temperatures, ranging from 650 to 750°C (1200 to 1400°F).

While the boiler operating conditions are important variables, the coal chemistry also plays a pivotal role in fireside corrosion. Some impurity constituents in coal are well known to cause boiler tube wastage.[2] For example, high sulfur and chlorine contents in coal have long been recognized as major contributors to fireside corrosion, especially on the waterwall and superheater/reheater tube surfaces. Other coal constituents, such as alkali, alkaline earth, and total ash content, also play an important role in fireside corrosion but are less understood. Indeed, operating experiences suggest that the corrosivity of coal is not just determined by individual impurities. Rather, it is the result of complex, synergistic effects from all of the coal impurities interacting with each others. There have been attempts in the past to link coal corrosivity to its impurities based on empirical correlations and indexing. However, the results proved to be less reliable and often coal-specific due to oversimplification of the interactions and/or significant variations in coal chemistry.

Coal typically contains a significant amount of sulfur. The impact of sulfur-containing gaseous species, such as H_2S, SO_2, SO_3, and COS, evolved from coal combustion on fireside corrosion has been discussed in the literature by Kung,[2] Kihara et al.,[6] Devito & Smith,[7] and Ivanova and Svistanova.[8] Furthermore, the original forms of sulfur in coal and their evolution have also been investigated extensively by Huffman et al.,[9] Calkins,[10] Kelemen et al.,[11] Gorbaty et al.,[12] LaCount et al.,[13] and Boudou et al.[14] A study was carried out by Bassilakis et al.[15] to determine the evolution of sulfur-containing species with a Fourier transform infrared spectrometer (FTIR) from eight coals selected for the Argonne Premium Coal Sample (APCS)

program. These authors concluded that sulfur in coal is present in three different forms, i.e., organic, pyritic, and sulfatic, where the latter is in a relatively small fraction.

Based on thermodynamic calculations, Chou et al.[16] predicted that coal-derived sulfur is released mostly as H_2S under substoichiometric combustion conditions. This prediction was in good agreement with the results of Bassilakis et al.[15] It should be mentioned that Bassilakis et al. measured the H_2S gas indirectly with the FTIR due to its weak infrared (IR) absorbance. The authors employed a post-oxidation technique, in which oxygen was supplied to the heated gas sampling stream after the combustion furnace and before the FTIR spectrometer to allow oxidation of the H_2S to form SO_2 (and H_2O). By monitoring the SO_2 evolution rate, the concentration of H_2S was calculated, assuming all of the measured SO_2 was converted from H_2S. From this study, it was found that approximately 50 percent of the coal sulfur was released from pyrolysis in the form of H_2S. The balance of the sulfur formed different sulfur-containing gas species, while some remained in tar and char.

Duan et al.[17] also performed a coal pyrolysis study with a FTIR and determined that pyritic sulfur initially became pyrrhotite ($Fe_{1-x}S$, where $0 \leq x \geq 0.2$) in inert atmospheres, followed by rapid reactions with hydrogen radicals to form H_2S during pyrolysis. In this study, the H_2S was measured directly with the FTIR despite its low IR absorbance. This study further revealed the mechanisms of H_2S formation from coal combustion. The accuracy of Duan et al.'s data could not be validated, as no similar FTIR measurements have been performed in the literature for comparison.

Attempts to model the amount of H_2S formation have been made by Kaminskii[18] who correlated the combustion of pulverized anthracite in various boilers with the amount of H_2S formed as a function of CO, SO_2, and excess air. Depending on local stoichiometry, the range of H_2S measured was up to 1400 ppm. Applicability of this model to coals other than anthracite is uncertain and needs to be further evaluated.

Srivastava et al.[19] reported that the concentration of SO_3 was typically in a small fraction (at ~1-2%) of the total SO_2 measured in a field study. Due to its low concentration, the total amount of sulfur in combustion gas can be approximated by the sum of other sulfur-containing gaseous species, e.g., H_2S, SO_2, and COS. It should be pointed out that, even though SO_3 is present in a relatively low quantity, it plays a pivotal role in fireside corrosion, especially coal ash corrosion in the upper furnace and dew point corrosion in the back end of coal-fired boilers.

Gaseous SO_2 and SO_3 can be measured by several techniques. Because the measurement methods for SO_2 are well established and routinely performed, they are not further discussed here. For SO_3, however, the measurement has proven to be quite challenging due to its high reactivity and tendency to condense as acid. Fukuchi and Ninomiya[20] measured SO_3 by means of ultraviolet absorption and thermal conversion (from SO_3 to SO_2). Himes[21] measured SO_3 using a FTIR spectroscopy with promising results. Jaworowski and Mack[22] reviewed a few techniques for the SO_3 measurement, including isopropyl alcohol, controlled condensation, and dew point determination. These authors concluded that none of the techniques were distinctly better, although the controlled condensation technique produced the most reliable results.

It should be mentioned that most of the studies available in the literature involved either thermodynamic calculations or pyrolysis of a relatively small coal sample in batch processing. Conditions produced from such laboratory-scale experiments are unlikely to resemble the dynamic combustion conditions produced in large coal-fired utility boilers. Therefore, the objective of this study was to determine the evolution and formation of sulfur and chlorine-containing gaseous species in a pilot-scale combustion facility. Online gas sampling and measurements were performed in the reducing and oxidizing zones of the test facility burning the selected coals individually in staged combustion. While many gaseous species were analyzed during the combustion tests, this paper focuses on the formation of sulfur and chlorine-bearing species of interest, including H_2S, S_2, SO_2, COS, SO_3, and HCl.

EXPERIMENTAL PROCEDURES

Combustion tests of the selected five coals were performed in a pilot-scale testing facility rated at 150 kW nominal thermal input. The facility, shown in Figure 1, is a down-fired, swirl-stabilized combustor with a chamber height of 265 cm and inner diameter of 75 cm. The combustion of each coal was staged by creating an average stoichiometric ratio (S.R.) of 0.85 in the burner zone (i.e., the top half of the combustor), followed by the injection of overfire air (OFA) to create an average S.R. of 1.15 in the bottom half of the chamber. The pilot-scale testing facility has many access ports for probe insertion, at approximately every 5 cm axially, thus allowing gas measurements at almost any location along the height of the combustion chamber.

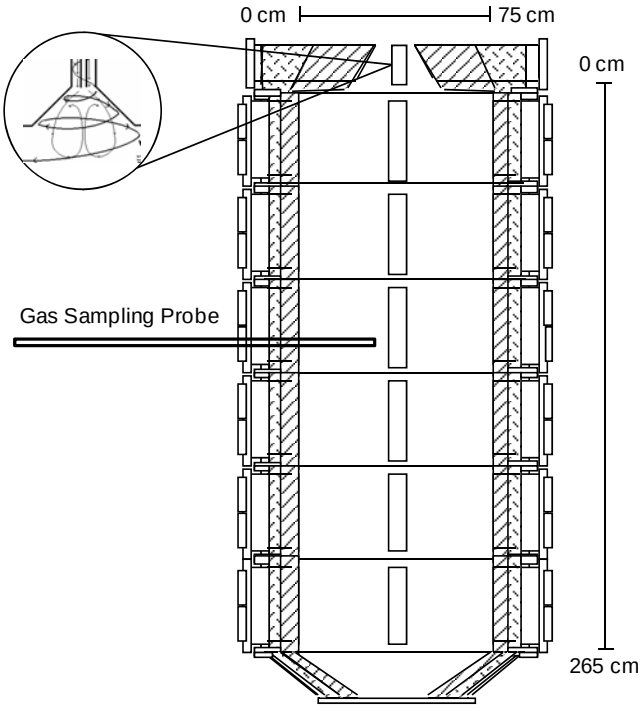

Figure 1 - Schematic Diagram of the Pilot-Scale Combustion Facility.

The proximate and ultimate analyses, heating values, and chlorine contents of the five coals investigated are listed in Table 1. Per ASTM classifications,[23] three of the coals are ranked as eastern bituminous, while PRB as sub-bituminous and Beulah Zap as lignite. The approximate locations of these coal mines in the U.S. are shown in Figure 2. The sulfur contents ranged from high (4.31%) in Gatling to low (0.25%) in PRB. All of these coals were processed and pulverized to a particle size of 70% passing 200 mesh and fired in the test facility at the same nominal heat rate (150 kW). Moisture is relatively high in the PRB and Beulah Zap lignite coals and low in the eastern bituminous. Due to their lower heating values, the fuel flow rates of PRB and lignite were adjusted higher than those of the bituminous coals during testing to achieve the desired thermal input.

The coal feeding system consisted of a bulk bag unloader and loss-in-weight feeder. After discharging from the bag, the pulverized coal was fed through an agitator hopper that filled the feeder hopper on demand. A pneumatic line was installed to convey the pulverized coal from the feeder to the burner. Such an integrated system allowed the coal feed rate to be maintained within 5% of the set point over a period of 1 minute and within 1% over a period of an hour. The feeder was also capable of maintaining a flow rate that fluctuated less than 5% from the set point during refill. Figure 3 is an overview of the coal feeding system.

Table 1
As-Received Ultimate and Proximate Analyses and Higher Heating Values for the Five Coals Studied. Chlorine is Listed on a Dry Basis.

Proximate	PRB	Beulah Zap	Indiana #6	Ill. #6 Galatia	Gatling
Moist.	24.59	27.33	7.25	3.68	3.77
Ash	5.14	8.66	7.20	10.45	11.34
Vol.	37.00	33.77	30.87	33.70	40.73
Carbon	33.27	30.24	54.68	52.17	44.16
Total	100.00	100.00	100.00	100.00	100.00
Ultimate					
Moist.	24.59	27.33	7.25	3.68	3.77
H	2.55	2.03	4.02	3.14	4.07
C	54.75	46.56	69.48	67.66	67.11
N	0.83	0.86	1.36	0.95	0.94
S	0.25	0.67	1.14	2.96	4.31
O	11.89	13.89	9.55	11.16	8.46
Ash	5.14	8.66	7.20	10.45	11.34
Cl (%Dry)	0.0012	0.001	0.2121	0.283	0.0387
HHV (Btu/lb)	9,156	7,792	12,400	12,464	12,191

Figure 2 – Approximate U.S. Locations of the Five Coal Mines Investigated.

Figure 3 –Coal Feed System Supplying Pulverized Coal to the Burner of Pilot-Scale Combustion Facility.

An online gas sampling system was developed to measure the concentrations of gaseous species formed in the reducing and oxidizing zones of the pilot-scale combustion facility. To prevent any loss of sampled gases from reactions inside the sampling line, the system was capable of quenching the hot gas samples rapidly from the combustion gas temperatures to the

line temperature while still maintaining the gas samples above the dew points of any condensable acids. Therefore, the entire sampling train, shown in Figure 4, consisted of a series of heated components controlled at 180°C at all times. All gas-touched surfaces in the sampling line were also constructed with either Teflon or Teflon-coated materials, as bare metal surfaces were found to react with the corrosive gases, such as H_2S, HCl, and SO_3, during the in-furnace gas measurements.

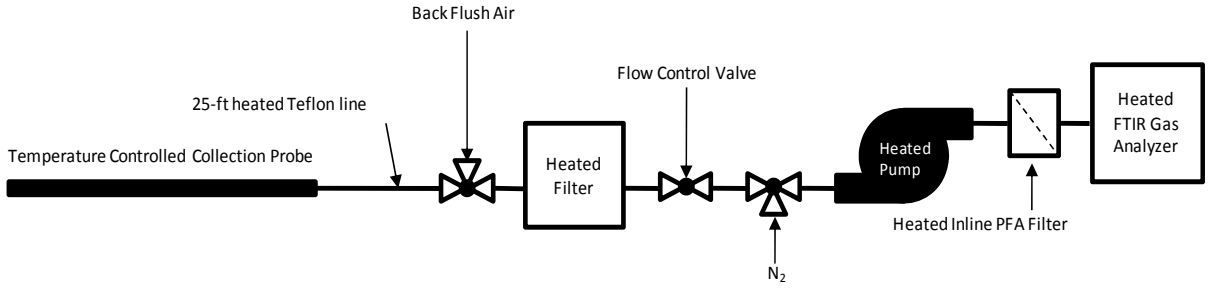

Figure 4 - Schematic of the Online Gas Sampling System Developed for the In-Situ Gas Measurement.

All gaseous species were measured with an online FTIR spectrometer equipped with a 5.11-m long pass gas cell. The maximum spectral resolution of the FTIR was 0.5 cm^{-1}. In the gas cell, where the IR light was passing through the sampled gases, the temperature was maintained at 150°C, slightly lower than that controlled in the sampling line. The implementation of a lower instrument temperature of 150°C was necessary due to the fact that the calibration curves available from the FTIR manufacturer were created at this temperature. However, this temperature should be sufficiently high to prevent any acids from condensing during the gas measurements.

Because H_2S has a weak FTIR absorbance spectrum, additional calibration for this gas was performed. The calibration involved feeding the FTIR with a calibration gas consisting of 817 ppm of H2S in nitrogen. With this calibration gas, any interference that might be introduced from other species was avoided, thus allowing a direct determination of the FTIR sensitivity to H_2S only. Subsequently, the FTIR was calibrated by sampling the flue gases generated in the oxidizing zone of the pilot-scale combustor where H_2S was negligible. Any H_2S detected from this zone was considered as signal noise.

From these calibration procedures, it was concluded that the noise in the FTIR measurements for H_2S could be as much as ±150 ppm at times. It was also determined that averaging the H_2S measurements over a period of approximately one minute (i.e., about 10 spectral scans) would reduce the data scattering to ± 50 ppm. If the gas cell optics became contaminated from particulates carried in the sampled gas stream, the FTIR signal would degrade, causing a lower signal to noise ratio for H_2S and thus higher uncertainty (up to ±100 ppm). Therefore, the resolution of FTIR for H_2S was not as good as all other gases analyzed. Nevertheless, the FTIR provided invaluable information on the evolution and formation of H_2S in this pilot-scale combustion study, which would be directly applicable to coal combustion in utility boilers.

RESULTS AND DISCUSSION

For better clarity, results of the online gas measurements for the reducing and oxidizing zones are discussed separately.

Gas Measurement in Reducing Zone

The gaseous species of interest, including H_2S, SO_2, SO_3, COS, CO, and O_2, were measured for each of the five coals in the reducing zone of the pilot-scale combustion facility, and the results are summarized in Tables 2-6. The concentration data are listed by the axial and radial locations of the sampling probe. "Rad" in the first column refers to the radial locations across the width of the combustor. Zero point of the radial location is at the wall opening through which the gas sampling probe was inserted. The probe traveled through the center of the combustor and eventually reached the opposite wall. The axial locations specified in the tables refer to the distance from the outlet of the coal injection tube in the burner, as shown in the inset of Figure 1.

The concentrations of CO and O_2 would serve as an indication of local stoichiometry at each sampling location. Detailed analysis of the measured gas concentrations is demonstrated here by using the Beulah Zap lignite in Table 3 as an example. The center of the combustor is at 37.5 cm from each wall. As shown in Figure 5, the measured concentrations of CO, H_2S, and COS from the lignite test exhibited a summit near the center of the combustor (i.e., ~30 cm), where the concentration of O_2 was at its lowest (not shown). Similar to O_2, the concentration of SO_2 was high near the walls (i.e., at the 10 and 60 cm positions) but low at the center.

The high CO concentrations measured near the center of the pilot-scale combustor indicate that a highly reducing zone was created by the incoming primary air-coal mixture. Meaningful amounts of free oxygen were detected by GC across the width of the combustor, as shown in Table 3. In particular, free oxygen was also detected at the center of the combustor where the local S.R. value was much lower than the overall 0.85. The presence of free oxygen (and unburned carbon) suggests that combustion in the burner zone was incomplete due to slow reactions between coal and air, which is typical for the lower furnace of coal-fired utility boilers.

Table 2
Measured Gas Concentrations for the PRB Coal under Reducing Conditions
S.R. = 0.85, Axial Distance = 90 cm

Rad. (cm)	CO (ppm)	H_2S (ppm)	SO_2 (ppm)	SO_3 (ppm)	COS (ppm)	O_2 (%)
10	5130	-41	190	11	7	4.35
20	5116	-81	179	12	6	4.08
30	6642	-27	171	11	7	3.46
40	38487	203	149	6	13	0.41
50	34866	180	141	7	13	0.66
60	15135	53	168	9	11	1.85
70	1835	-35	149	10	7	4.33

Table 3
Measured Gas Concentrations for the Beulah Zap Lignite Coal under Reducing Conditions
S.R. = 0.85, Axial Distance = 77 cm

Rad. (cm)	CO (ppm)	H_2S (ppm)	SO_2 (ppm)	SO_3 (ppm)	COS (ppm)	O_2 (%)
10	11617	54	781	12	20	2.89
20	39181	170	629	15	71	0.90
30	47406	571	298	13	108	0.96
40	42536	465	419	10	75	0.86
50	29380	98	666	19	45	1.26
60	6640	-107	719	18	21	3.01
70	1030	-91	668	19	11	3.36

Table 4
Measured Gas Concentrations for the Indiana #6 Coal under Reducing Conditions
S.R. = 0.85, Axial Distance = 70 cm

Rad. (cm)	CO (ppm)	H_2S (ppm)	SO_2 (ppm)	SO_3 (ppm)	COS (ppm)	O_2 (%)
10	4922	-48	936	23	-9	2.36
20	23160	-73	1025	20	16	0.71
30	43060	146	674	14	42	0.51
40	45558	135	743	11	12	0.41
50	37564	305	797	16	18	0.51
60	16239	-27	1237	30	0	0.56
70	10105	-76	1133	26	-2	0.63

Table 5
Measured Gas Concentrations for the Illinois #6 Galatia Coal under Reducing Conditions
S.R. = 0.85, Axial Distance = 83 cm

Rad. (cm)	CO (ppm)	H_2S (ppm)	SO_2 (ppm)	SO_3 (ppm)	COS (ppm)	O_2 (%)
10	1297	-99	1891	44	1	4.79
20	47745	436	1410	24	49	0.63
30	55010	710	990	19	-8	0.34
40	28671	380	2128	43	43	0.52
50	1901	-65	2221	54	-1	3.66
60	731	50	2038	48	2	4.14
70	522	-8	1887	45	4	4.66

Table 6
Measured Gas Concentrations for the Gatling Coal under Reducing Conditions
S.R. = 0.85, Axial Distance = 63 cm

Rad. (cm)	CO (ppm)	H_2S (ppm)	SO_2 (ppm)	SO_3 (ppm)	COS (ppm)	O_2 (%)
10	16759	134	2763	64	98	0.06
20	24322	249	2405	65	124	0.02
30	29285	693	2343	51	57	0.01
40	26573	801	2342	58	71	0.00
50	13329	280	3374	58	53	0.05
60	4234	70	4250	81	4	0.29
70	4131	2	3549	76	3	0.63

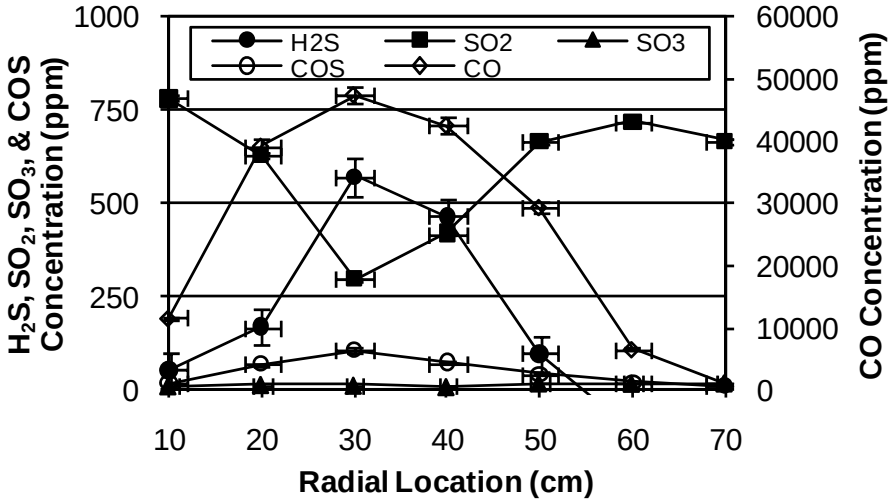

Figure 5 - Total Concentration of H_2S, SO_2, SO_3, and COS Measured Across the Burner Zone of Pilot-Scale Combustion Facility for Beulah Zap Lignite

The concentration profiles of H_2S and COS followed closely with that of CO, with the highest values present at the center of the combustor and the lowest near the walls. Where the H_2S and COS concentrations were high, the SO_2 and O_2 concentrations were low. Such trends are consistent with the thermodynamic prediction for sulfur-bearing gaseous species. The SO_3 concentration was relatively low compared to the other sulfur species, typically in the order of 2-3 percent of the total sulfur-containing gases.

It should be mentioned that, in spite of the coal groups, all of the gas concentrations given in Tables 2-6 exhibited similar trends to those discussed for Beulah Zap lignite, i.e., with a strong reducing zone near the center of the combustor and relatively oxidizing regions close to the walls. The coexistence of measurable amounts of reducing and oxidizing gases in the burner zone, along with unburned carbon across the width of the combustor, is a strong indication of non-equilibrium in the combustion gases despite different degrees of local substoichiometry. The lack of thermodynamic equilibrium is again consistent with what is generally observed in commercial boilers. Such results imply that the environments for fireside corrosion in coal-fired utility boilers should not be predicted solely by means of thermodynamic calculations. In-furnace gas measurement should also be considered as a viable tool.

The total concentrations of sulfur-containing gases, including H_2S, SO_2, COS, and SO_3, measured for the five coal groups are shown in Figure 6 as a function of the radial position in the reducing zone of the pilot-scale testing facility. In general, variation in the total sulfur-containing gaseous species appeared to be small across the width of burner zone, with a deviation typically less than 10 percent of the mean values. Among them, the Illinois #6 and Gatling coals, which consist of higher coal sulfur contents, exhibited a slightly greater variation in the total sulfur concentrations. The lack of a large variation in total sulfur suggests that coal was distributed quite uniformly across the width of the combustor during each combustion test. The uniform distribution of fuel was primarily achieved by the swirling capability of the burner with

secondary air, an important feature that closely resembles full-scale commercial burners in coal-fired utility boilers.

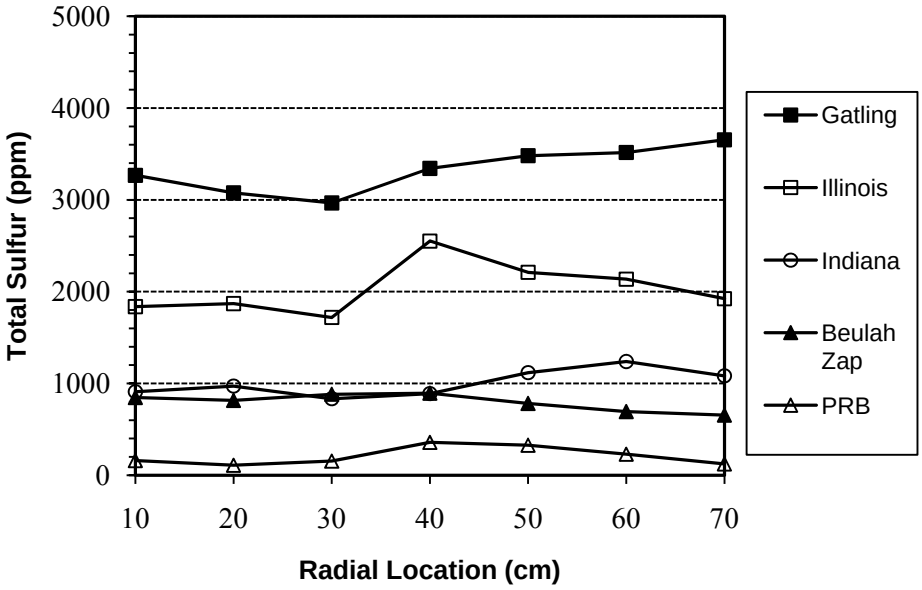

Figure 6 - Total Concentrations of H_2S, SO_2, SO_3, and COS Measured for Different Coals

Table 7 compares the averaged concentrations of four sulfur-bearing gaseous species (H_2S, SO_2, SO_3, and COS) that could be measured by FTIR across the combustor width in the reducing zone to the total coal sulfur contents of the five coal groups. Note that the total sulfur species listed does not include S_2, even though its presence in the gas phase at the combustion temperatures is not insignificant. The S_2 gas is non-polar; therefore, it cannot be detected by FTIR. Consequently, the S_2 gas cannot be included for comparison here. Furthermore, there are two batches of Illinois #6 Galatia coal investigated. Due to a noticeable difference in composition, both batches, designated as 6-1 and 6-2, are included in Table 7 and treated as two different coals.

Table 7
Comparison of Coal Sulfur with Total Measured Sulfur-Containing Species.

Coal	Total Coal Sulfur, As Received (wt.%)	Avg. Total Sulfur, Measured* (ppm)
PRB	0.25	219
Beulah Zap	0.67	846
Indiana #6	1.14	954
Illinois #6-1	2.69	2534
Illinois #6-2	2.96	2319
Gatling	4.31	3388

*** Including H_2S, SO_2, SO_3, and COS but not S_2.**

Table 7 shows that the averaged concentration values of the four sulfur-bearing gases across the combustor width in the reducing zone trended closely with the amounts of sulfur in coal. The averages of the measured concentrations for the four sulfur-bearing gaseous species were further compared to those predicted by thermodynamic calculations performed using a commercial code (HSC version 5.1) at the S.R. of 0.85 and 1200°C, as shown in Table 8. This temperature was selected because it represents the typical gas temperature in the lower furnace of coal-fired utility boilers outside of the fireball (or flame).

Table 8
Comparison of Sums of Four Measured and Calculated Sulfur-Containing Species.

Coal	Total Measured Sulfur Species* Excluding S_2 (ppm)	Total Calculated Sulfur Species* Excluding S_2 at 1200°C (ppm)
PRB	219	358
Beulah Zap	846	1018
Indiana #6	954	1090
Illinois #6-1	2534	2163
Illinois #6-2	2319	2520
Gatling	3388	3355

*** Including H_2S, SO_2, SO_3, and COS but not S_2.**

The information in Tables 7 and 8 are graphically presented in Figure 7 by plotting the averages of total measured and calculated concentrations of the four sulfur-bearing species (H_2S, SO_2, SO_3, and COS) as a function of total sulfur content in coal. Again, despite its meaningful presence, the S_2 gas cannot be included in the comparison due to the limitation of online measurement by FTIR (or any other measuring techniques) for non-polar gases.

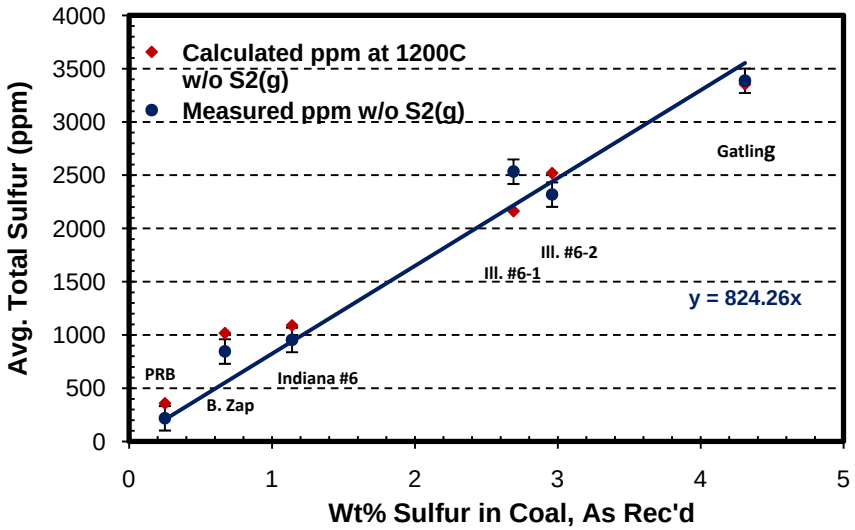

Figure 7 - Comparison of the Sums of Four Measured and Calculated Sulfur-Bearing Gases (H_2S, SO_2, SO_3, and COS), Excluding S_2, in the Reducing Zone for Different Coals across the Combustor Chamber.

Figure 7 shows that the sums of both measured and calculated concentrations for the four sulfur-bearing gases are in a linear relationship with the total sulfur content in coal. The figure also reveals an excellent agreement between the measured and calculated total concentrations of the four sulfur-bearing gases in the reducing zone. Based on thermodynamic calculations, only metal oxides are stable as a condensed phase under the combustion conditions of interest, which can then condense on the furnace walls. Unlike oxides, no condensed sulfur-containing phases are expected to form at 1200^{o}C. The excellent agreement between the measured and calculated values suggests that, despite different coal sulfur forms, essentially all of the sulfur in coal is rapidly released to the gas phase at the combustion temperatures. This finding is contrary to the general speculation that some sulfur in coal, especially present in the pyritic and sulfatic forms, would remain largely unreacted during combustion and subsequently deposited on the waterwalls. Results from this study do not support such a speculation, as the release of coal sulfur and reaction to form gaseous species appear to be instantaneous.

However, sulfur is commonly found in the deposit samples collected from utility boilers. The sulfur-containing compounds existing in the deposit samples are probably formed as a result of secondary reactions between the deposit and combustion gases. Mechanistically, all sulfur in coal is first released to the gas phase during combustion and form different gaseous species. In the meantime, metal oxides are also stable in the combustion gases and can be physically thrown to the furnace walls to form deposit. Subsequent exposure of the oxides in the deposit to the combustion gases at much lower temperatures (due to the low waterwall temperatures) allows the conversion of condensed oxides to sulfur compounds.

To estimate the amounts of S_2 present in the gas phase, the total sulfur concentrations of the four sulfur-bearing species (H_2S, SO_2, SO_3, and COS) measured in the reducing zone are compared to the total sulfur concentrations of five sulfur-bearing species (including S_2) predicted by thermodynamic calculations, as shown in Figure 8. Again, the comparison is made by plotting the total sulfur concentrations as a function of coal sulfur content. Thermodynamically, the five sulfur-containing gases, i.e., H_2S, S_2, SO_2, SO_3, and COS, predicted by the calculations would account for all of the sulfur in the coal. Therefore, difference in the measured and calculated total sulfur concentrations in Figure 8 is attributed to S_2.

Figure 8 indicates that approximately 24% of coal sulfur is present in the gas phase as S_2. Among the coal groups studied, the partial pressures of S_2 in the combustion gases can span in two orders of magnitude, ranging from $5x10^{-6}$ atm. for PRB to $6x10^{-4}$ atm. for Gatlin. These levels of partial pressures are much higher than those calculated based simply on the S.R. and coal chemistry at the furnace wall temperatures, as typically reported in the literature. The presence of high partial pressures of S_2 in the gas phase further supports the proposed mechanism of secondary reactions mentioned above. At low temperatures and high partial pressures of S_2 on the waterwalls, some metal oxides in the deposit become less stable than the corresponding sulfides. For example, iron oxide (Fe_3O_4) is formed from pyrite (FeS_2) in coal during combustion after the release of sulfur. The iron oxide is then thrown to the furnace walls and becomes part of the deposit constituents. Upon subsequent exposure of the deposit to the combustion gases having a high partial pressure of S_2, the iron oxide is no longer stable at the furnace wall temperatures and may quickly be converted to iron sulfide (FeS). Such a mechanism may explain frequent observation of FeS in the deposit.

It should be mentioned that results of this study reveal the coexistence of both S_2 and O_2 in the combustion gases. Such a phenomenon is again an indication of non-equilibrium in the overall combustion gases, even though the release and reaction of sulfur appear to be fast, approaching partial equilibrium among the sulfur-bearing species.

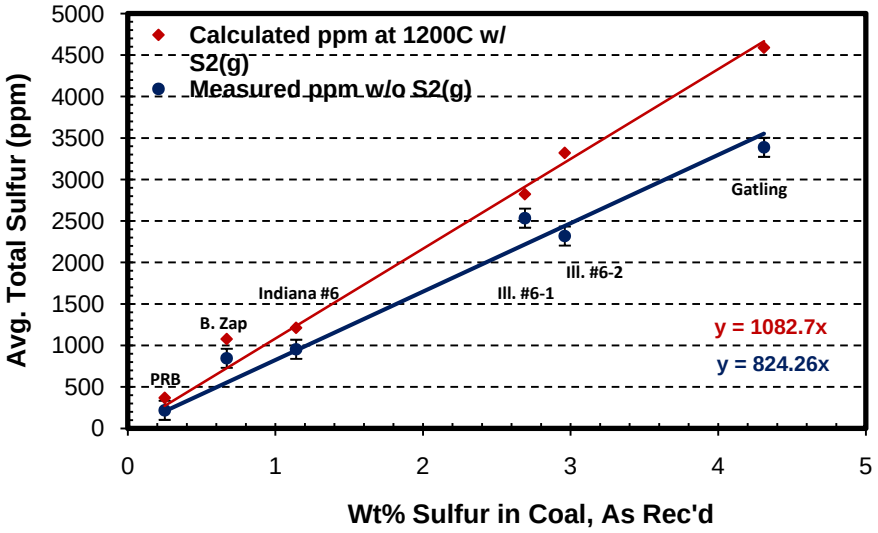

Figure 8 – Comparison of the Measured Concentrations of Four Sulfur-Bearing Species (Excluding S_2) to Calculated Concentrations of Total Sulfur Species (Including S_2) for Different Coals at 1200°C.

The concentrations of HCl were also measured across the burner zone with the FTIR for the coals studied. Unlike the other gaseous species, the concentrations of HCl only varied slightly with the probe locations, with the highest readings obtained near the center of the combustor and lowest near the walls. The averaged HCl concentrations measured at all locations across the burner zone were compared to the total chlorine contents in coal, as shown in Figure 9, The HCl concentrations predicted by thermodynamic calculations at 1200°C are also included in the plot. Because of the low chlorine contents of PRB and Beulah Zap lignite, the averaged HCl concentrations measured from the combustion tests were negligible. Despite its very high sulfur content, the Gatling coal had a relatively low chlorine concentration, thus reflected by the low HCl average in Figure 9 as well. Both Indiana #6 and Illinois #6 contained high chlorine concentrations. As a result, the measured HCl concentrations in the combustion zone were much higher.

The concentrations of HCl, both measured and calculated, also varied with the coal chlorine content in a near linear relationship, as shown in Figure 9. However, unlike sulfur, the measured HCl concentrations amount to about 80% of the calculated values at 1200°C. The unreacted chlorine did not condense in the deposit. Instead, as will be discussed in the next section, it continued to be released and fully converted to HCl in the oxidizing zone. Discrepancy in the measured and calculated HCl concentrations indicates that the release of chlorine from coal during combustion is relatively slower than that of sulfur.

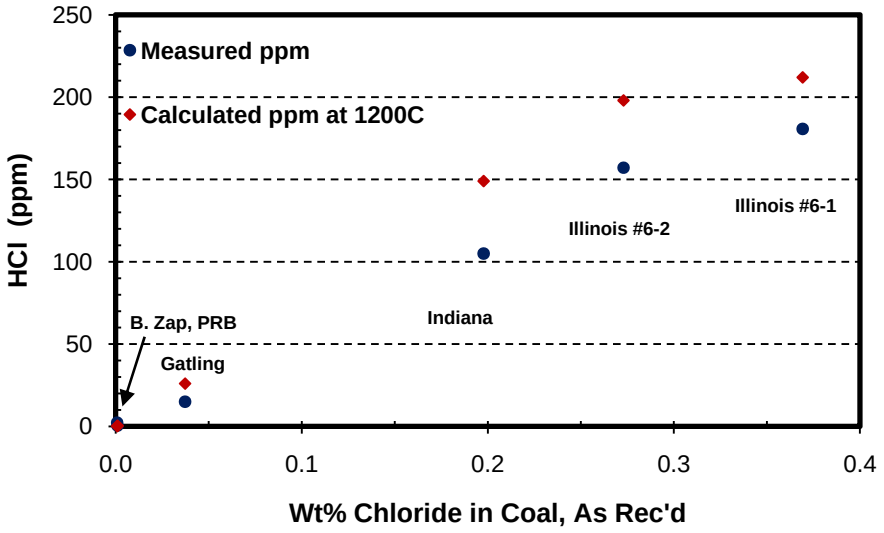

Figure 9 – Comparison of Measured and Calculated HCl Concentration in the Reducing Zone for Different Coals as a Function of Coal Chlorine Content.

Gas Measurement in Oxidizing Zone

In general, concentrations of the measured gaseous species in the oxidizing zone were relatively constant across the lower chamber of the pilot-scale combustion facility. Again, the small variation in concentrations indicated a uniform distribution of the fuel. Rather than listing the position-specific information, the averaged gas concentrations measured at all locations for the coals are summarized in Table 9. For ease of comparison, the coals are listed in the order of increasing sulfur content. The concentrations of both SO_2 and SO_3 increased with increasing coal sulfur. Similar to the reducing zone, the ratio of SO_3 to SO_2 for the coals also remained constant at approximately 2-3%. The slightly higher ratio observed for the PRB coal was likely attributed to measurement limitations, as a very low concentration of SO_3 was detected by the FTIR.

Table 9
Averaged Gas Concentrations Measured in Oxidizing Zone for Different Coals

Coal	CO (ppm)	H_2S (ppm)	SO_2 (ppm)	SO_3 (ppm)	O_2 (%)	SO_3/SO_2 Ratio
PRB	30	13	154	8	2.6	0.05
Beulah Zap	22	202	556	10	3.0	0.02
Indiana	543	-9	854	26	3.5	0.03
Illinois #6	478	-14	2065	45	2.8	0.02
Gatling	179	-5	2983	68	3.3	0.02

At a S.R. of 1.15, the oxygen concentration would be approximately 3% in the oxidizing zone. The measured O_2 concentrations for these coals were indeed near this level, ranging from

2.6 to 3.5%. The CO concentrations were very low in the oxidizing zone compared to those for the reducing regions listed in Tables 2-6. However, some CO, even though at very low concentrations, was still detectable, especially for the Indiana and Illinois coals. The presence of CO indicates incomplete combustion of the coals even in a highly oxidizing environment, which again highlights the non-equilibrium nature of the combustion gases. The H_2S concentrations for the coals scattered between negative and positive values in the oxidizing zone. Due to the measurement uncertainty of ±50 ppm associated with signal interference from moisture in the FTIR as discussed previously, most of the H_2S values should be considered nil. One exception is the Beulah Zap lignite that appears to have produced a measurable amount of H_2S in the oxidizing zone.

The average sums of both measured and calculated concentrations of sulfur-containing gases in the oxidizing zone are summarized in Figure 10 as a function of the coal sulfur content. Similar to the reducing zone, a linear relationship between the total sulfur in the gas phase (primarily as SO_2) and total sulfur in coal is evident. Such a relationship once again suggests that the amount of sulfur released from coal to the gas phase and form gaseous species in the oxidizing zone is proportional to the amount of total sulfur in coal, independent of the sulfur forms. Furthermore, the total concentrations of sulfur species measured and calculated for the coals in the oxidizing zone are in good agreement. Such an agreement is expected because all of sulfur in coal has already been released to the gas phase in the reducing zone upstream of the oxidizing region, as discussed previously. Like the reducing zone, secondary reactions between deposit and the combustion gases may be responsible for the formation of metal sulfates on the boiler (superheater) tubes at lower temperatures.

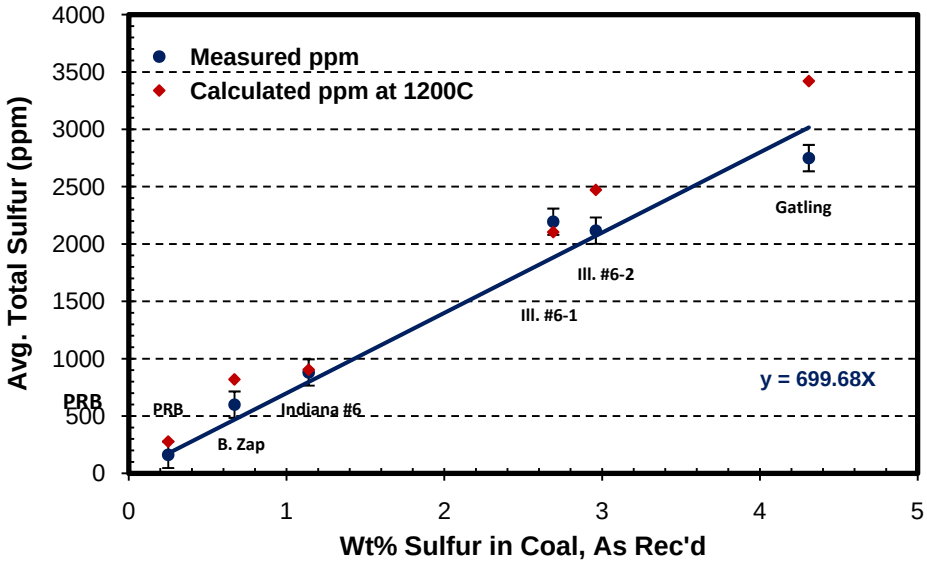

Figure 10 - Comparison of Measured and Calculated Total Sulfur in the Gas Phase of Oxidizing Zone for Different Coals as a Function of Total Coal Sulfur Content.

The concentrations of HCl were also measured across the oxidizing zone of the pilot-scale combustion facility with the FTIR. Similar to the reducing zone, the concentrations of HCl

remained relative constant at different probe traverse locations. The HCl concentrations across the oxidizing zone were averaged and compared to the total chlorine contents in the coal, as shown in Figure 11. In addition, the HCl concentrations predicted by thermodynamic calculations at 1200°C are also included in the comparison.

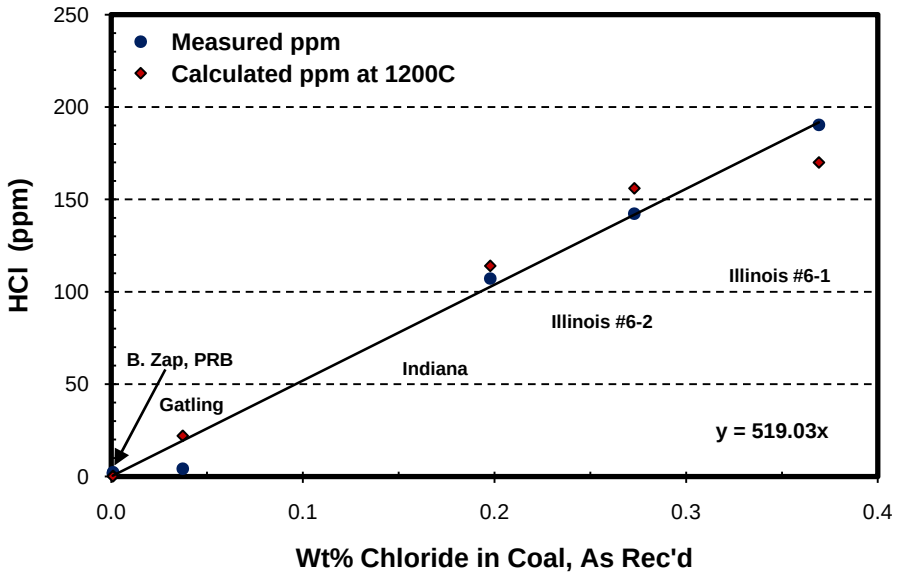

Figure 11 - Comparison of Measured and Calculated HCl Concentrations in the Oxidizing Zone for Different Coals as a Function of Total Coal Chlorine Content.

Figure 11 shows that the concentrations of measured HCl are in good agreement with those predicted by thermodynamic calculations at 1200°C. As a result, the discrepancy observed in the reducing zone, shown in Figure 9, has vanished. Such results suggest that the unreacted chlorine in the reducing zone must have stayed in the combustion gases, perhaps as a constituent of the suspended coal particles, and continued to be released. As the combustion gases travelled from the reducing zone to oxidizing zone, estimated to be within one second, a sufficient time was provided to complete the release of chlorine and conversion to HCl. Had the chlorine condensed out in the deposit upstream of the oxidizing zone, the concentrations of HCl measured at this location would have remained lower than the values predicted by thermodynamic calculations. Results of this study indicate that a rapid release of coal chlorine also takes place during combustion, although the process is slightly slower than that of sulfur.

CONCLUSIONS

The formation of sulfur and chlorine-containing gaseous species from burning five U.S. coals has been investigated in a fireside corrosion study. The coals consisted of a wide range of chemistry that is of interest to the utility industry. These coals were pulverized and burned in a pilot-scale combustion facility to closely simulate the actual conditions of staged combustion in commercial coal-fired utility boilers. During each of the combustion tests, gas samples were collected and analyzed via in-furnace probing in the combustion facility at various locations

corresponding to the lower furnace walls and superheaters. The gas compositions were determined in-situ with online instrumentations, including FTIR, GC and Horiba multi-gas analyzer.

The in-furnace gas measurements revealed the coexistence of reducing and oxidizing species in the gas phase, evincing the non-equilibrium nature of the overall combustion products. While the concentrations of individual gaseous species varied across the chamber of the combustor, average concentrations of the total sulfur and chlorine-containing gases remained relatively constant. Such a small variation in total sulfur and chlorine indicates a uniform distribution of the fuel achieved across the combustor during testing. Furthermore, the amounts of sulfur and chlorine released to form sulfur-bearing gaseous species in both the reducing and oxidizing zones were in a linear relationship with the amount of total sulfur and chlorine in coal, independent of their original forms. The release of sulfur from coal during combustion appeared to be instantaneous, resulting in near equilibrium of the sulfur-containing species in the gas phase, even though overall equilibrium of the combustion gases was not attained. Chlorine was also released rapidly to form HCl. However, the kinetics of chlorine release and reaction appeared to be slightly slower than those of sulfur.

Because all sulfur in coal was accounted for in the gas phase at the combustion temperatures, no condensable sulfur compounds would be formed directly from coal combustion. However, sulfur is commonly found in deposit samples collected from utility boilers, especially in the form of sulfides and sulfates. It is proposed that the sulfur compounds detected in the deposit would be the result of secondary reactions between metal oxides in the deposit and sulfur-containing flue gases. For example, the secondary reactions can promote the formation of FeS from the original Fe_3O_4 formed during coal combustion and deposited on the furnace walls. The presence of FeS in the deposit has been linked to accelerated sulfidation attack on the waterwalls under certain operating conditions. The secondary reactions can also result in the formation of sulfates on superheaters, leading to coal ash corrosion. Similarly, all the chlorine in coal was present in the gas phase as HCl. Results of thermodynamic calculations indicate that the concentrations of HCl generated from coal combustion are insufficient to convert metal oxides in the deposit to chlorides under normal boiler operating conditions. Therefore, the fireside corrosion associated with chlorine is likely to be caused by gas-solid reactions between HCl and the boiler tube alloys. The information generated from this study on sulfur and chlorine release is vital to the understanding of fireside corrosion mechanisms and helps improve the design of laboratory tests to better simulate the fireside conditions of coal-fired utility boilers.

ACKNOWLEDGEMENT

This work was supported by the U.S. Department of Energy under Award Number DE-FC26-07NT43097. The author would like to acknowledge the DOE project manager, Vito Cedro, at the National Energy Technology Laboratory in Pittsburgh, PA, for his collaboration.

REFERENCES

1. R. Viswanathan, R. Purgert, and U. Rao, "Materials Technology for Advanced Coal Power Plants," Journal of Materials Engineering and Performance, Vol. 14, No. 3, June 2005.
2. S. C, Kung, "Fireside Corrosion in Coal- and Oil-Fired Boilers," ASM Handbook, 13C, 2006.
3. S. C. Kung, "Prediction of Corrosion Rate for Alloys Exposed to Reducing/Sulfidizing Combustion Gases," Materials Performance, Vol. 36, No. 12, pp. 36-40, 1997.
4. S. C. Kung, "Effect of Iron Sulfide on Furnace Wall Corrosion," ERPI Report No. TR-111152, 1998.
5. R. A. Rapp and Y. S. Zhang, "Hot Corrosion of Materials: Fundamental Studies," Journal of Metals, Vol. 46, No. 12, pp. 47-55, 1994.
6. S. Kihara, K. Nakagawa, A. Ohtomo, H. Aoki, and S. Ando, "Simulating Test Results for Fireside Corrosion of Superheater and Reheater Tubes Operated at Advanced Steam Condition in Coal-Fired Boilers." High Temperature Corrosion in Energy Systems, 361-376, 1985.
7. M. S. DeVito and D. L. Smith, "Controlled Condensation Method: New Option for SO3 Sampling." Power, 135(2), 1991.
8. I. P Ivanova and L. A. Svistanova, "Corrosion of 12Kh1MF Steel and Different Corrosion-Resistant Coatings in an Atmosphere of Flue Gases when Burning Anthracite Culm." Thermal Engineering (English Translation of Teploenergetika), (1), 60-63, 1971.
9. G. P. Huffman, S. Mitra, F. E. Huggins, N. Shah, S. Vaidya, and F. Lu, "Quantitative Analysis of All Major Forms of Sulfur in Coal by X-ray Absorption Fine Structure Spectroscopy." *Energy & Fuels*, 5, 574-581, 1991.
10. W. H. Calkins, "Investigation of Organic Sulfur-containing Structures in Coal by Flash Pyrolysis Experiments." *Energy & Fuels*, 1, 59-64, 1987.
11. S. R. Kelemen, G. N. George, and M. L. Gorbaty, "Direct Determination and Quantification of Sulphur Forms in Heavy Petroleum and Coals 1. The X-ray Photoelectron Spectroscopy (XPS) Approach." *Fuel*, 69(8), 939, 1990.
12. M. L. Gorbaty, G. N. George, and S. R. Kelemen, "Direct Determination and Quantification of Sulphur Forms in Heavy Petroleum and Coals 2. The Sulphur K Edge X-ray Absorption Spectroscopy Approach." *Fuel*, 69(8), 945, 1990.
13. R. B. LaCount, D. K. Walker, R. B. Lacount Jr., R. K. Walker, A. L. Stewart, T. K. Trulli, D. G. Kern, D. J. Miltz Jr., and W. P. King, "Advances in Coal Characterization by Programmed-temperature Oxidation." *Fuel*, 72(8), 1203-1208, 1993.
14. J. P. Boudou, M. Nip, J. J. Boon, J. Boulegue, J. W. de Leeuw, and L. Malechaux, "Identification of Some Sulphur Species in a High Organic Sulphur Coal." *Fuel*, 66(11) 1558-1569, 1987.
15. R. Bassilakis, Y. Zhao, P. R. Solomon, and M. A. Serio, "Sulfur and Nitrogen Evolution in the Argonne Coals: Experiment and Modeling." *Energy & Fuels*, 7(6), 710-720, 1993.
16. S. F. Chou, P. L. Daniel, and A. J. Blazewicz, "Hydrogen Sulfide Corrosion in Low-NO_x Combustion Systems." *Journal of Materials for Energy Systems*, 7(4), 361-369, 1986.
17. L. Duan, C. Zhao, W. Zhou, C. Qu, and X. Chen, "Investigation on Coal Pyrolysis in CO_2 Atmosphere." *Energy & Fuels*, 23(7), 3826-3830, 2009.

18. V. P. Kaminskii, “The Mechanism of How Several Components of the Flame Form and Act on the Tube Metal of the Waterwalls of Power Boilers when Burning Anthracite Culm.” Thermal Engineering, 43(6), 505-510, 1996.
19. R. K. Srivastava, C. A. Miller, C. Erickson, and R. Jambhekar, “Emissions of Sulfur Trioxide from Coal-fired Power Plants.” Journal of the Air & Waste Management Association, 54(6), 750-762, 2004.
20. T. Fukuchi and H. Ninomiya, “SO3 Concentration Measurement Using Ultraviolet Absorption Spectroscopy and Thermal Conversion.” IEEJ Transactions on Fundamentals and Materials, 126(10), 977-982, 2006.
21. R. Himes, “Keeping an Eye on SO3.” Power Engineering, 110(4), 24-32, 2006.
22. R. J. Jaworowski and S. S. Mack, “Evaluation of Methods for Measurement of SO3/H2SO4 in Flue Gas.” Journal of Air Pollution Control Association, 29(1), 43-46, 1979.
23. ASTM Standards, “Standard Classification of Coals by Rank,” D388-95, 1995.
24. McBride, B.J., & S. Gordan, (1994). *Computer Program for Calculation of Complex Chemical Equilibrium Compositions and Applications*. Cleveland, Ohio, USA, Lewis Research Center, pts. I.
25. McBride, B.J., & S. Gordan, (1996). *Computer Program for Calculation of Complex Chemical Equilibrium Compositions and Applications*. Cleveland, Ohio, USA, Lewis Research Center, pts. II.